STRUCTURE, NANOMECHANICS AND INFECTION DYNAMICS OF SINGLE VIRUS PARTICLES

PhD thesis

Bálint Kiss

Doctoral School of Theoretical and Translational Medicine

Semmelweis University

Supervisor: Miklós Kellermayer, MD, D.Sc

Official reviewers: Péter Galajda, Ph.D
Orsolya Dobay, Ph.D

Head of the Complex Examination Committee: Alán Alpár, MD, D.Sc

Members of the Complex Examination Committee: László Cervenák, Ph.D
Mihály Kovács, D.Sc

Budapest

2022

1. Introduction

While it is often debated whether viruses can be considered living organisms, in my view they are nature's "nanorobots" evolved to carry out a single function. Their main goal is to reprogram the host cell for viral reproduction. Viruses are comprised of a shell and a viral genome and can infect either eukaryotic or prokaryotic cells. Their infection cycle is closely intertwined with that of the host, and they can only reproduce through the complex process of infection. Their structure has evolved to achieve the most efficient genome delivery into their target, the mechanism of which can greatly vary among the different viral species. In my thesis, I will present our recent findings on the structure and infection cycle of T7 and SARS-CoV-2.

SARS-CoV-2 is an enveloped single-stranded ribonucleic acid (ssRNA) virus with a corona-shaped layer of spike proteins, which play a crucial role in host recognition, and virus entry (Fig. 1). Structural information about the spike protein has been acquired either on crystals of purified protein or on fixed and frozen virus particles. It has been suggested that the spike hinges provide structural flexibility, which might increase host-recognition efficiency. High-resolution cryogenic electron microscopy (cryo-EM) observations indicate that the ribonucleoprotein (RNP) of SARS-CoV-2 is partitioned into spherical, basketlike structures. These small spherical structures composed of RNA and proteins fill the viral particle. However, the surface dynamics and mechanical properties of native virions remain to be understood.

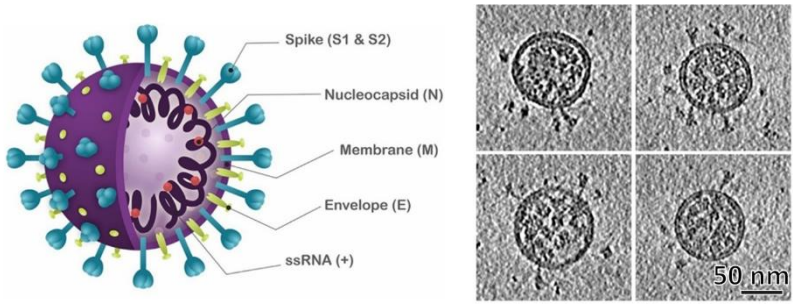

Fig. 1. Schematics and cryo-EM images of SARS-CoV-2. *Schematics of a SARS-CoV-2 particle (left), and four representative cryo-EM images of SARS-CoV-2 particles adapted from Ke et al. (right).*

In contrast to SARS-CoV-2, bacteriophages are regarded as a convenient model system, since working with them is not as hazardous as in the case of human pathogens. T7 bacteriophages are double-stranded DNA viruses comprised of an icosahedral capsid with an internal protein core (which is unique to T7) and a short non-contractile tail (Fig. 2).

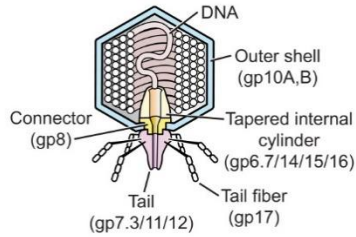

Fig. 2. Schematic structure of the T7 bacteriophage.

This tail-fiber complex enables the phage to bind to its target and deliver its genome into the host. Although the structure and properties of T7 have been investigated extensively, our knowledge of its host-recognition and DNA injection mechanisms remain very incomplete.

In my thesis I will explain studies employing atomic force microscopy (AFM) and molecular force spectroscopy, which we used to investigate the topographical and nanomechanical properties of native SARS-CoV-2 virions, and to visualize individual host-cell bound T7 phages. Furthermore, fluorescence microscopy was utilized to visualize the target binding and DNA ejection process of T7 phages.

2. Objectives

Our long-term goal is to better understand viral structure which is closely related to the nanomechanical processes that control infection. Viral infection can be separated into three phases: target recognition, viral reproduction and finally the release of viral progeny. We aim to understand the first and final phases of infection by fluorescent labeling and AFM scanning, thereby observing the process of host recognition, docking and DNA release.

Our detailed goals and focuses are the following:

- Understanding the global structure and nanomechanics of SARS-CoV-2 virions.
- Investigating SARS-CoV-2 thermal stability.
- Understanding the target recognition and docking process of T7 bacteriophages.
- Uncovering the exact mechanisms of T7 DNA ejection.
- Exploring infection-induced global structural changes and lysis of the target bacterium.

3. Methods

SARS-CoV-2 sample preparation for AFM studies

Purified SARS-CoV-2 particles were pipetted onto anti-spike antibody covered surfaces. Such functionalized substrates greatly enhanced the binding affinity of viral particles, thereby increasing the number of surface bound viruses. In case of native samples, the AFM scanner was transported to the BSL-3 facility of the National Biosafety Laboratory. After loading the sample into the scanner, it was sealed and brought back for imaging to the Biophysics and Radiation Biology Department of Semmelweis University. In case of fixed samples, 5 % glutaraldehyde was used to inactivate the viruses.

T7 bacteriophage binding studies

Bacterial cells were dropped onto poly-L-lysine coated coverslips (TIRF/phase-contrast imaging) or mica surfaces (AFM imaging). T7 bacteriophages were pipetted onto surface adhered bacteria to initiate phage-host interaction studies. In case of TIRF microscopy measurements bacteriophages were labeled with Sytox Orange (SyO) DNA intercalator dye. In case of fixed samples, 5 % glutaraldehyde was used to fix samples.

T7 DNA ejection experiments

Bacteriophages were bound to a glass bottom microfluidic flow cell through which the sample was observed by TIRF microscopy. The DNA of bacteriophages was labeled with SyO fluorescent dye.

AFM imaging and force spectroscopy

AFM imaging was carried out with an Asylum Research Cypher ES instrument. Scanning was performed in liquid at 20 °C either in phosphate buffered saline (SARS-CoV-2 and T7 samples) or in liquid broth (T7 infection of *E. coli* cells), in non-contact mode with BL-AC40TS (Olympus) cantilevers. Cantilevers were oscillated by BlueDrive technology

(photothermal excitation) at an average free amplitude of 0.5 V, 350 mV setpoint, near the resonance frequency of the cantilevers, usually around 20 kHz. Force spectroscopy was carried out on targeted virions in contact mode, by lowering the cantilever with 0.5 µm/s velocity until the typical set force of 2 nN was reached. Spring constant of BL-AC40TS cantilevers varied between 90-120 pN/nm. Image post-processing and analysis were performed by using the AFM driving software (IgorPro, WaveMetrics).

4. Results

4.1. SARS-CoV-2

Structure of fixed SARS-CoV-2 particles

The structure and topographical surface of SARS-CoV-2 particles was revealed by AFM. Viral particle immobilization was facilitated by antibody-enhanced affinity binding onto the surface. Antibody-mediated binding was necessary to increase the number of surface-adhered particles, as well as to increase the specificity of surface binding, thereby increasing the purity of the sample to be scanned (Fig. 3A).

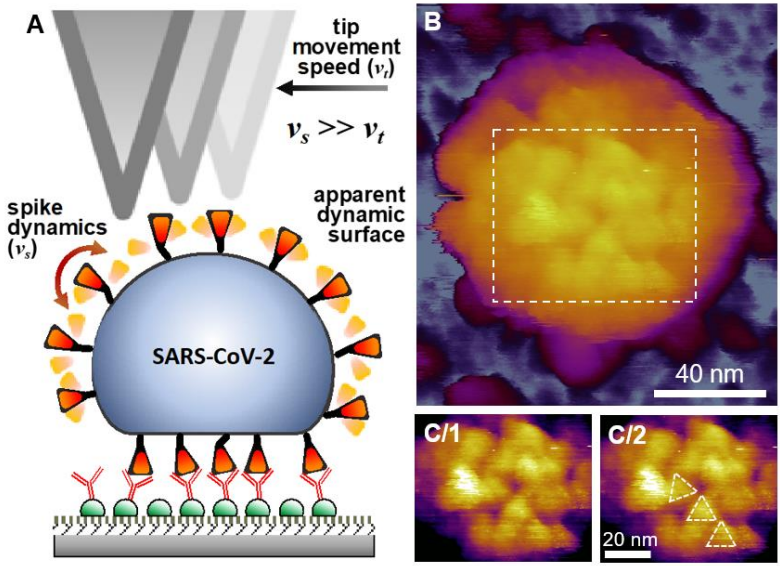

Fig. 3. Topographical structure of SARS-CoV-2 virions treated with 5 % glutaraldehyde for structural preservation. *(A) Schematics of scanning substrate-surface-bound virions with the AFM tip. (B) High-resolution AFM image of a SARS-CoV-2 virion displaying axial view of S trimers. (C/1) Enlarged and contrast-enhanced image of the rectangular area marked by white dashed line in B. (C/2). The same AFM image with overlaid triangles indicating S trimer orientation.*

Affinity-enhanced surfaces increased the number of SARS-CoV-2 particles hundred-fold. Chemical fixation by glutaraldehyde was necessary due to safety reasons as well as to increase the strength of surface binding, thereby improving topographical resolution. These high-resolution scans revealed individual SARS-CoV-2 viruses bound on to the substrate surface (Fig. 3B). Analysis of surface-bound particles had variable heights and diameters (62 ± 8 nm). SARS-CoV-2 particles were identified by their tetrahedral spike-trimers visualized by AFM (Fig. 3C).

Nanomechanics of SARS-CoV-2

Apart from imaging, AFM can also be utilized to mechanically probe a sample, thereby providing unique structural and mechanical information. Following non-contact mode scanning, which allows the localization of individual viral particles, we have performed multiple nanomechanical indentation cycles on the viruses (Fig. 4A).

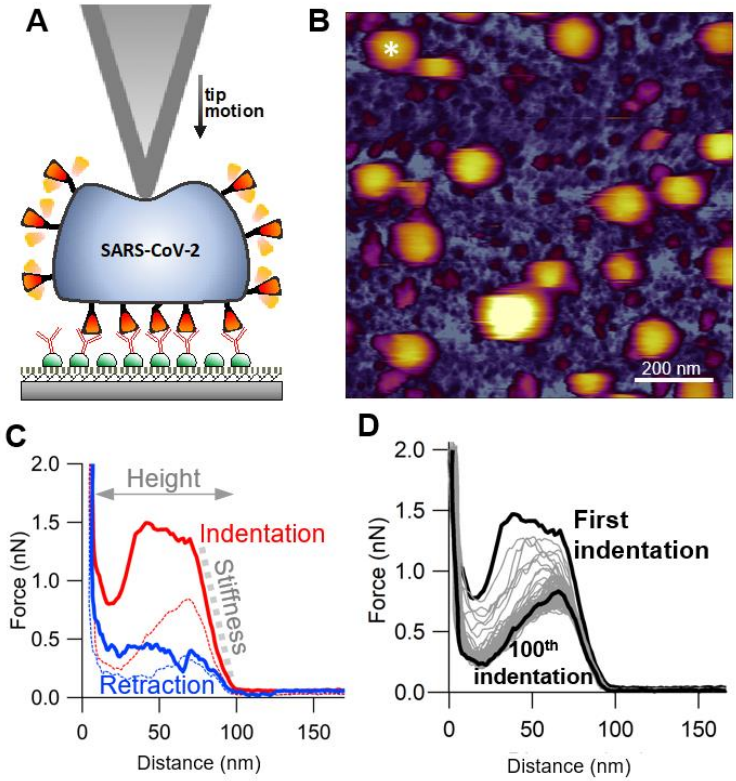

Fig. 4. Single-particle force spectroscopy of SARS-CoV-2 virions. *(A) Schematics of the force-spectroscopy experiment. The virion is indented with the AFM tip until a pre-set force (typically 2-3 nN) is reached. (B) AFM image of an overview (1 x 1 µm) sample area prior to nanomechanical manipulation. Asterisk shows a virion selected for nanomechanical manipulation. (C) Example of a force versus distance curve obtained during a single indentation-retraction cycle. From the slope of the indentation curve (gray dotted line) and the distance between the landing point and substrate limit of the trace we obtained the stiffness and the force-spectroscopic height of the virions, respectively. Red and blue dotted lines indicate indentation and retraction data, respectively, obtained in the 100th nanomechanical cycle. (E) Force versus distance curves obtained during repeated indentation of a single SARS-CoV-2 virion.*

Virus indentation was performed with a constant velocity of 0.5 µm/s on individual viral particles (Fig. 4B) until a preset level of force was reached

(typically 2-3 nN). The mean force-spectroscopical height was 94 ± 10 nm (n = 40), which is comparable to that obtained from topographical data. Remarkably, the virions could be compressed wall-to-wall. By surprise, the severe nanomechanical indentation did not result in visible topographical changes. The indentation cycle could be partitioned into multiple stages. Initially, landing on the virion is followed by an elastic compression phase, the steepness of which corresponds to the stiffness of the virions (Fig. 4C). The mean stiffness of the virions was 13 ± 5 pN/nm (n = 40). The linear compression region is then followed by a yield point at which the virion structure suddenly changes. From this point onward, internal force-induced structural transitions take place until total wall-to-wall compression occurs, after which the tip immediately hits the substrate surface. Following complete indentation and upon reaching the preset force limit the cantilever is retracted. Interestingly, the virion exerted forces on the cantilever on the magnitude of several hundreds of piconewtons during the retraction cycle, which means that internal rearrangement of the previously disrupted structure is taking place against force. Such forces were present until the height of the previously indented particle was reached. Indentation cycles could be repeated up to 100 times. However, and to our surprise, apart from a slight fatigue, the virions never broke or collapsed (Fig. 4D). Indentation and retraction cycles relaxed after a couple dozens of cycles, then the hysteresis decreased.

4.2. T7 bacteriophage

T7 explores the *E. coli* surface for binding site

To follow the target recognition kinetics and DNA translocation process of bacteriophages, their DNA was labelled with SyO by allowing the dye to penetrate the capsid shell. Docked bacteriophages appeared as bright fluorescent particles along the edge of the bacterium (Fig. 5A). Phage binding

to *E. coli* was isotropic, as we could not observe any directional or spatial preference. To reveal the surface dynamics of individual phage particles, we tracked the position of the fluorescent spots as a function of time. In the early stages of infection, bacteriophages that retained their genomes long enough to be observed for several minutes moved around randomly on the target cell surface (Fig. 5AB). Although phage movement occasionally accelerated and eventually stopped altogether (Fig. 5B), initial periods of random motion with a more-or-less constant velocity were well discernible. The displacement of the phage particles from their landing point as a function of time (Fig. 5C) could be fitted with a power function with fractional exponent, suggesting diffusive motion. At room temperature, the random target search proceeded for several minutes (Fig. 5CD). The total travel path grew linearly and could reach up to 5 μm (Fig. 5D). The mean slope of this function, thus the average speed of exploration was ~10 nm/s. To test whether the target search is free diffusion, we measured, with identical analytical tools, the two-dimensional diffusion of polystyrene beads with radii similar to that of T7's. The average speed of bead motion was nearly two orders of magnitude greater than that of target search by T7. Thus, target search is a diffusive motion the speed of which is limited, most likely, by reversible interactions between the virus and the host cell surface.

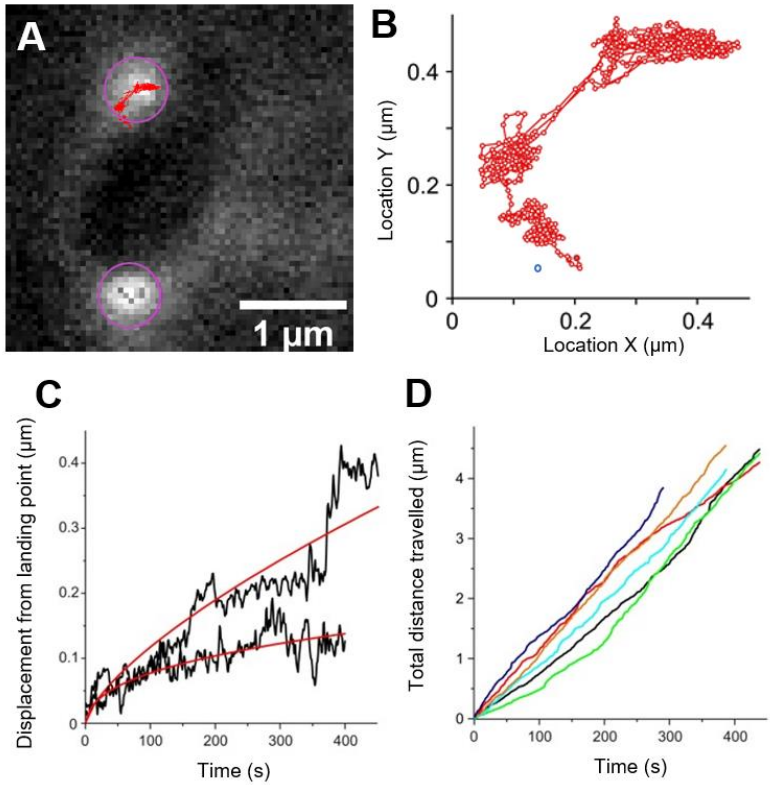

Fig. 5. Phages travel on the bacterial surface. *(A) Bacteriophages searching on the surface of a bacterium. Purple circles show tracked particles; red line shows the trajectory of the upper particle. (B) Enlarged graph of the trajectory shown in A/1, blue spot shows the initial binding point. (C) Black curves show the distance of two tracked viruses from their landing point over time, red line shows a parabolic function fitted to the data. (D) Total distance traveled by tracked phages from their initial binding point. Different colors correspond to different viruses.*

Photothermally induced DNA release of T7

To investigate the DNA ejection of T7 bacteriophages *in vitro*, we investigated single-phage particles immobilized in a microfluidic device and monitored the appearance of DNA by SyO labeling using TIRF microscopy (Fig. 6A).

In the beginning of the experiment the field of view was dark, and bright spots corresponding to single T7 virions started to appear with a lag time due to *in situ* labeling with SyO (Fig. 6B). After an average lag time of 21 ± 12 s (n = 34) viral DNA was ejected into the medium, where it was immediately stretched out in parallel to the flow direction. DNA ejection was a rapid process, and more than half of the genome was ejected within a fraction of a second (0.13 ± 0.07 s). Remarkably, DNA ejection was never complete on the experimental time scale, and most of the viral genome (84 ± 5%; n = 134) remained attached to the capsid throughout the observation period (Fig. 6C). 82 % of DNA ejections halted after 80 % of the genome has been released.

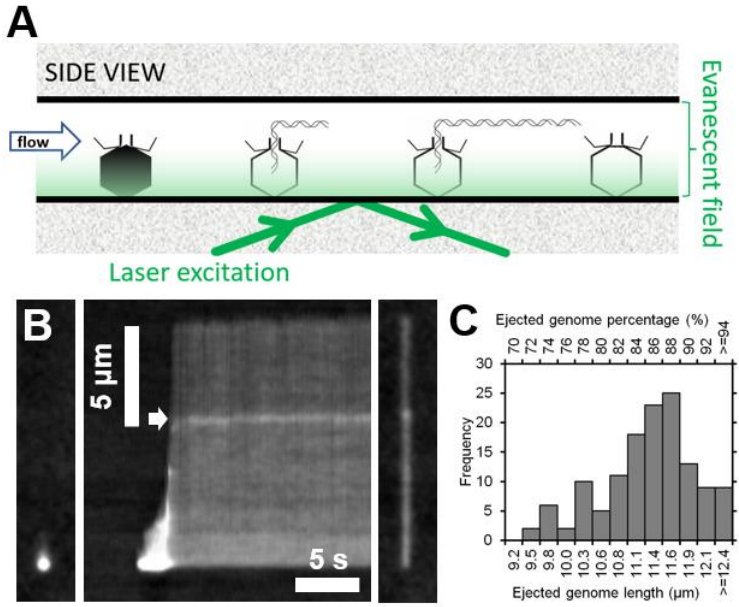

Fig. 6. Bacteriophage DNA ejection in solution. (A) Experimental setup of single-phage DNA ejection assay. (B) Images (left and right), and kymograph (middle) of a bacteriophage ejecting its DNA. (C) Distribution of ejected genome fractions. White arrow points to a more intensely labeled region of DNA.

5. Conclusions

The atomic force microscopic imaging and nanomechanical measurements revealed that the SARS-CoV-2 virion is spherical, highly dynamic, compliant, and resilient, and it displays remarkable mechanical and global thermal stabilities. Unfixed, native state measurements revealed a blurred viral surface, which we attribute to rapid spike movements. While the dynamics of the surface spikes may play an important role in the unusually high infectivity of the virus, its mechanical and self-healing properties may also ensure adaptation to a wide range of environmental circumstances. Although SARS-CoV-2 particles are resilient in case of sharp tip indentation, plateau tip compression induces irreversible structural changes.

Viral infection comprises a highly complex series of interconnected and synchronized events. T7 binds reversibly to the *E. coli* surface which it explores for the proper binding site by diffusive motion. It has been postulated that lipopolysaccharide (LPS) is a primary receptor for T7, however we could not confirm these results. By employing TIRF and AFM the docking process of single T7 phages can be observed. Our results suggest that the exploratory motion of T7 entails the rolling of the phage on the bacterial surface rather than walking with the fibers. Phage docking is initiated by binding of the tail to its receptor, and the fibers are involved in capsid positioning for rapid (~1 min) and efficient genome transfer. DNA release can be triggered *in vitro* by a photothermal mechanism which leads to partial genome ejection that stops short of the lysis-related genes, pointing at the presence of a mechanical genome-transfer control. At high excitation levels bleaching derived reactive oxygen species can possibly damage the capsid structure and cause the viral DNA to leak out from multiple points. The T7 infection ends with a violent cell lysis preceded by bacterial membrane surface roughening and bleb

formation. Single virus observations such as the ones employed in this work can greatly contribute to the general understanding of nature's nanomachines.

Novel, thesis-related findings:

1) Native SARS-CoV-2 particles display a blurred surface as observed by AFM, which is related to rapid spike movements.
2) SARS-CoV-2 is highly resilient mechanically and can recover from multiple sharp tip indentation cycles. SARS-CoV-2 is among the most elastic viral nanoparticles.
3) The global structure of SARS-CoV-2 remains unchanged during heating cycles up to 90°C, however spikes dissociate from the viral surface.
4) T7 bacteriophages bind to their target cells in a reversible manner.
5) We suggest that target bound bacteriophages are not "walking" but exploring the host cell surface by a non-specific adhesion mediated rolling process.
6) DNA injection is a rapid (1 min) process, whereby most of the genome (~90%) is transferred into the target cell.
7) In the presence of certain DNA intercalators T7 genome ejection can be photothermally triggered by high laser excitation levels.
8) Photothermally triggered DNA release is incomplete, 80% of DNA ejections halt after ejecting ~82% of the genome.

6. Bibliography of the candidate's publications

Publications related to the thesis

1. Kiss, B., Kis, Z., Pályi, B., & Kellermayer, M. S. (2021). Topography, spike dynamics, and nanomechanics of individual native SARS-CoV-2 virions. Nano letters, 21(6), 2675-2680.
2. Kiss, B., Kiss, L. A., Lohinai, Z. D., Mudra, D., Tordai, H., Herenyi, L., ... & Kellermayer, M. (2022). Imaging the Infection Cycle of T7 at the Single Virion Level. International Journal of Molecular Sciences, 23(19), 11252.

Unrelated publications

Research Articles

1. Padányi, R., Farkas, B., Tordai, H., Kiss, B., Grubmüller, H., Soya, N., ... & Hegedűs, T. (2022). Nanomechanics combined with HDX reveals allosteric drug binding sites of CFTR NBD1. Computational and Structural Biotechnology Journal.
2. Kellermayer, D., Kiss, B., Tordai, H., Oláh, A., Granzier, H. L., Merkely, B., ... & Radovits, T. (2021). Increased expression of N2BA titin corresponds to more compliant myofibrils in athlete's heart. International journal of molecular sciences, 22(20), 11110.
3. Kiss, B., Bozó, T., Mudra, D., Tordai, H., Herényi, L., & Kellermayer, M. (2021). Development, structure and mechanics of a synthetic E. coli outer membrane model. Nanoscale Advances, 3(3), 755-766.
4. Máthé, D., Kiss, B., Pályi, B., Kis, Z., Forgách, L., Hegedűs, N., ... & Kellermayer, M. S. (2021). The 3M Concept: Biomedical

Translational Imaging from Molecules to Mouse to Man. The EuroBiotech Journal, 5(3), 155-160.

5. Forgách, L., Hegedűs, N., Horváth, I., Kiss, B., Kovács, N., Varga, Z., ... & Máthé, D. (2020). Fluorescent, Prussian Blue-Based Biocompatible Nanoparticle System for Multimodal Imaging Contrast. Nanomaterials, 10(9), 1732.
6. Kiss, B., Mudra, D., Török, G., Mártonfalvi, Z., Csík, G., Herényi, L., & Kellermayer, M. (2020). Single-particle virology. Biophysical Reviews, 12(5), 1141-1154..
7. Kretzer, B., Kiss, B., Tordai, H., Csík, G., Herényi, L., & Kellermayer, M. (2020). Single-Molecule Mechanics in Ligand Concentration Gradient. Micromachines, 11(2), 212..
8. Hegedűs, N., Forgách, L., Kiss, B., Varga, Z., Jezsó, B., Horváth, I., ... & Máthé, D. (2022). Synthesis and preclinical application of a Prussian blue-based dual fluorescent and magnetic contrast agent (CA). PloS one, 17(7), e0264554.